Received: 17 June 2025 | Revised: 11 August 2025 | Accepted: 5 September 2025

DOI: 10.1002/suco.70330

ARTICLE

fib CEB-FIP WILEY

A review on the behavior of FRP-reinforced ultra-high-performance concrete tubes

Rami J. A. Hamad[1] | **Mustafa Maher Al-Tayeb**[2] | **Bassam A. Tayeh**[3,4] | **Majed A. A. Aldahdooh**[1] | **Nurdeen M. Altwair**[5] | **Abdullah M. Zeyad**[6]

[1]International College of Engineering and Management, Muscat, Oman

[2]Department of Civil Engineering, Faculty of Engineering, Hasan Kalyoncu University, Gaziantep, Şahinbey, Turkey

[3]Islamic University of Gaza, Gaza Strip, Palestine

[4]Department of Civil & Environmental Engineering, University of Waterloo, Waterloo, Ontario, Canada

[5]Civil Engineering Department, Faculty of Engineering, Elmergib University, Khoms, Libya

[6]Civil Engineering, College of Engineering, Jazan University, Jazan, Saudi Arabia

Correspondence
Bassam A. Tayeh, Department of Civil & Environmental Engineering, University of Waterloo, Waterloo, ON, Canada.
Email: btayeh@iugaza.edu.ps

Abstract

This paper reviews previous research on ultra-high-performance concrete (UHPC) tubes confined with fiber-reinforced polymer (FRP). It summarizes current studies and provides insights for future research. UHPC-filled FRP tubes with different fiber types and tube thicknesses were tested to investigate their mechanical properties. It focuses on how different FRP types and numbers of FRP layers affect failure modes, mechanical properties, energy absorption, and ductility. Generally, the specimens failed by rupture of the tube at or near the midheight. Similar to conventional concrete, test results showed significant enhancements in the ultimate strength and strain of UHPC compared with its unconfined counterpart. For the same level of FRP confinement, the highest increase in ultimate strength is observed in CFRP-confined UHPC columns, as CFRP has higher stiffness compared to other FRP types such as AFRP and GFRP. The paper also examines models used to simulate experimental results, helping to understand UHPC behavior under FRP confinement better.

KEYWORDS

confined tubes, fiber-reinforced polymer, ultra-high-performance concrete

1 | INTRODUCTION

Fiber-reinforced polymer (FRP) composites are strong, lightweight materials that enhance the structural performance of concrete structures.[1–4] Their ability to improve compressive ductility has made FRP confinement a common method for strengthening normal-strength concrete (NSC).[5–23] Extensive research has been conducted on the compressive behavior of FRP-confined NSC and HSC.[24–35] Different researchers have developed design models to predict the stress–strain behavior for FRP-confined NSC.[36–39] Later, these models were revised by others to include partially confined NSC.[36–39] Both models demonstrate a high level of accuracy in predicting the stress–strain behavior of fully and partially FRP-confined NSC. However, these models did not provide accurate predictions for FRP-confined HSC as the axial stress–strain behavior of FRP-confined HSC differs from that of FRP-confined NSC. The post-peak stress reductions in FRP-confined HSC are primarily due to the brittle nature of HSC[40–42] and its low dilation tendency, which reduces the effectiveness of FRP confinement in maintaining its strength after failure.[40]

2 | ULTRA-HIGH-PERFORMANCE CONCRETE

Ultra-high-performance concrete (UHPC) is an advanced cementitious material. It has superior mechanical properties such as ultra-high strength, high toughness, and

excellent durability, which make it a better option than traditional concrete.[43–62] Several studies have explored various aspects of UHPC, including its mix proportions, curing methods, and mechanical properties such as compressive and tensile strength.[63–69] UHPC has exceptional properties compared with NSC and HSC, which make it an attractive alternative option for structural applications, particularly in bridge construction.[70–72] Although UHPC has improved ductility over HSC, it still needs lateral confinement to improve the post-peak ductility and toughness.[73,74] UHPC allows for the design of smaller cross sections in structural elements compared to traditional concrete.[75] UHPC has unique microstructural characteristics, high spalling resistance, high ability to form multiple microcracks, high bond strength, and excellent deformability. These superior properties make UHPC highly suitable for seismic applications.

Unlike traditional concrete, which includes both fine and coarse aggregates, UHPC contains ultra-fine particles. These ultra-fine particles fill the spaces between other larger particles, leading to a denser microstructure. This dense microstructure enhances the mechanical properties of UHPC. This high compactness results in greater density, fewer defects, and lower permeability compared to conventional concrete.[46] Additionally, incorporating steel fibers in UHPC can further enhance concrete strength by restraining the development of micro-cracks, resulting in significantly higher compressive and tensile strength compared to those of normal concrete.[76,77]

Similar to FRP-confined plain concrete[12–20,34,35] and FRP-confined reinforced concrete,[78–85] the axial compressive strength of UHPC can be greatly improved through full wrapping UHPC with FRP jacketing. Several studies have investigated the axial compressive behavior of FRP-confined UHPC, and this paper provides a comprehensive review of these findings.

However, this paper reviews previous research on UHPC tubes confined with FRP. It summarizes current studies and provides insights for future research. UHPC-filled FRP tubes with different fiber types and tube thicknesses were tested to investigate their mechanical properties.

3 | EXPERIMENTAL PROGRAM

Zohrevand and Mirmiran[86] carried out the initial experimental investigation into the compressive behavior of UHPC with a 2% volume fraction of steel fibers (unconfined compressive strength = 189 MPa). The UHPC was placed inside carbon FRP (CFRP) and glass FRP (GFRP) tubes, each with a concrete core with a diameter of 108 mm and a height of 191 mm. Subsequent studies investigated the effect of FRP confinement on UHPC concrete cylinders, taking into consideration different parameters such as cylinder size, UHPC mix proportions, UHPC strength, FRP type, FRP thickness and number of layers, and test type. The findings from different studies are summarized in Tables 1 and 2.

The experimental parameters outlined in this study align with the ranges presented in Table 5, enabling a direct and meaningful comparison of confinement effectiveness, failure modes, and energy dissipation characteristics across the reviewed studies.

4 | FAILURE MODES AND BEHAVIOR OF FRP-CONFINED UHPC

Zohrevand and Mirmiran[86] observed that all FRP-confined UHPC specimens failed due to sudden rupture of the FRP tube at or near mid-height. The GFRP tubes exhibited sequential rupture of inner layers, whereas CFRP tubes ruptured simultaneously at the mid-height, then the tube began to unzip along its length. Figure 1b,c shows the typical failure of specimens with glass and carbon FRP tubes, respectively.

Guler[87] and Tian et al.[90] similarly reported that unconfined UHPC failed in a brittle manner, with a rapid drop in load after reaching the peak load. In contrast, FRP-wrapped specimens showed a more progressive failure, with cracking noises heard before failure. CFRP- and Aramid FRP (AFRP)-wrapped UHPC columns experienced a gradual failure process, culminating in a sudden and explosive rupture. GFRP-wrapped UHPC columns failed more gradually, with significantly less explosiveness than CFRP and AFRP, indicating their higher post-peak stability. Before failure, cracking noises and the expansion of white patches on the outer surface of the FRP tube were observed, caused by the lateral dilation of UHPC. The severity of rupture increased with FRP thickness and higher confinement ratios, reflecting the instantaneous release of accumulated strain energy. All specimens failed with a sudden FRP rupture and explosion; however, failure modes varied depending on FRP type and tube thickness, with thicker tubes and CFRP producing more explosive behavior, and thinner tubes or GFRP showing more gradual failure. Specimens with partially longitudinally aligned fibers (60°) demonstrated a more progressive failure compared to those with fully transverse fibers (80°), highlighting the effect of fiber orientation on post-peak ductility and failure control.

Guler,[87] Tian et al.,[90] and Liao et al.[92] observed that FRP failure typically initiated away from the overlap region at mid-height and propagated toward the specimen's ends. Liao et al.[92] further highlighted the influence

TABLE 1 Experimental program.

Author	Diminution		UHPC strength (kN)	FRP types	FRP thickness	FRP tensile strength (kN)	No. of layers	Test types
	Dia.	*h*						
Zohrevand and Mirmiran[86]	108	191	1882	CFRP	1.02	3790	2, 4	Axial stress–strain
				GFRP	1.02	2275	2,3,4,5	
Guler[87]	100	200	1250	CFRP	0.35	3950	2, 3, 4, 5	Axial stress–strain
				GFRP	0.35	2790	2, 3, 4, 5	
				AFRP	0.32	2930	2, 3, 4, 5	
Deng and Qu[88]	100	200	828	AFRP	0.19	2000	-	Axial stress–strain
				BFRP	0.34	3103	-	
				CFRP	0.17	3400	-	
				GFRP	0.44	1800	-	
				A + BFRP	0.53	1079	1, 2, 3	
				B + GFRP	0.78	863	1, 2, 3	
				C + BFRP	0.51	1045	1, 2, 3	
				C + GFRP	0.60	1067	1, 2, 3	
				C2A1G1 FRP	0.69	980	-	
				C2A2G2 FRP	1.59	1010	-	
				C2B1G1 FRP	1.11	791	-	
				C2B2G2 FRP	1.88	823	-	
Wang et al.[89]	150	300	1188 without fiber	CFRP	0.17	2471	1, 3, 5	Axial stress–strain
				GFRP	0.17	1582	5	
	150	300	1749 with fiber	CFRP	0.17	2471	1, 2, 3, 5	
				GFRP	0.17	1582	3, 5, 9	
Tian et al.[90]	100	200	1154	GFRP Winding angle 60°	1	462	2, 5	Axial stress–strain
				Winding angle 80°	1	649	2, 5	
			1312 hot curing	Winding angle 80°	1	601	2, 5	
de Oliveira et al.[91]	50	100	1610	CFRP	0.17	3420	1, 2, 4	Axial stress–strain
				GFRP	0.13	1670	1, 2, 4	
			2040 heat curing	CFRP	0.17	3420	1, 2, 4	
				GFRP	0.13	1670	1, 2, 4	
Liao et al.[92]	50	100	1500	CFRP	0.17	-	1, 2, 3	Axial stress–strain
				GFRP	0.43	-	4, 6, 8	
	100	200	1400	CFRP	0.17	-	1, 2, 3	
				GFRP	0.43	-	4, 6, 8	
Ding et al.[93]	242	500	1324	CFRP 20 mm stirrups spacing		2058	-	Axial stress–strain
				CFRP 35 mm stirrups spacing			-	
				CFRP 50 mm stirrups spacing			-	
			1388	GFRP 20 mm stirrups spacing		1098	-	
				GFRP 35 mm stirrups spacing			-	
				GFRP 50 mm stirrups spacing			-	

(Continues)

TABLE 1 (Continued)

Author	Diminution		UHPC strength (kN)	FRP types	FRP thickness	FRP tensile strength (kN)	No. of layers	Test types
	Dia.	*h*						
Huang et al.[94]	100	50	1150	CFRP	0.167	4338	1, 2, 3	Split Hopkinson pressure bar impact load
Tian et al.[95]	150	300	1250	CFRP	0.167	3721	3, 4, 6	Load with constant eccentricity (0, 10, 20, and 30)
Wang et al.[96]	100	200	1365	CFRP	0.167		2, 3, 4, 5	Axial stress–strain
				GFRP	0.167		3, 5	
	150	300	1365	CFRP	0.167		3, 5	
Li et al.[97]	150	300	1085 without fiber 1222 with fiber	CFRP	0.167	3340	1 layer with spacing 60, 40, 20, and 0 cm	Axial stress–strain
Wang et al.[98]	240	500	1300 without fiber 1450 with fiber	GFRP	4, 6	746	Inner steel tube with 203 mm diameter and 6 mm thickness	Axial stress–strain

of specimen size on failure mode. They found that in smaller CFRP/GFRP-wrapped specimens (50 mm diameter), failure occurred in the hoop direction at mid-height, whereas in larger specimens (100 mm diameter), failure followed the fiber winding direction.

Deng and Qu[88] investigated the failure behavior of unconfined and hybrid-FRP (HFRP) confined UHPC. The study found that unconfined UHPC remains initially in the elastic stage, then exhibited longitudinal cracks at 30% of ultimate load, which extended and grew rapidly with increasing load, causing outward expansion at mid-height and increased hoop deformation at 75% of ultimate load. At ultimate load, vertical or diagonal cracks propagated throughout the specimen, causing brittle failure, though the structure maintained overall good integrity. HFRP-confined UHPC demonstrated multi-stage failure with delayed rupture, as lateral expansion gradually activated the confinement. At 90% of the ultimate load, a transverse crack formed in the HFRP tube, followed by fracturing sounds and mid-height bulging. At ultimate load, the tube cracked at mid-height, with cracks spreading toward the ends. Unlike single-type FRP confinement, which often failed explosively, hybrid FRP confinement allowed gradual energy dissipation and improved post-peak behavior.

Wang et al.[89] compared the failure behavior of ultra-high-performance fiber-reinforced concrete (UHPFRC) with UHPC without fibers. They found that plain UHPC exhibited significant cracking and spalling as it approached its strength limit, leading to explosive failure with the loss of concrete segments. However, UHPFRC failed due to the formation of vertical cracks running along the entire height of the specimen. The failure of UHPFRC was sudden and occurred either through the pulling out or rupture of the steel fibers under tension. However, no concrete loss was observed, which helped maintain the structural integrity of the UHPFRC. These results confirm that steel fibers effectively restrain crack propagation and spalling, which reduces the brittleness of UHPFRC and prevents the explosive failure. This demonstrates that steel fibers stabilize the core, reduce brittleness, and improve post-peak integrity.

Wang et al.[89] also explored the behavior of FRP-confined UHPC specimens with and without steel fibers. The unreinforced FRP-confined UHPC specimens exhibited sudden and explosive failure, characterized by the hoop rupture of the FRP jacket and the concrete core splitting into multiple segments. The severity of this explosive behavior intensified as the number of FRP layers increased, reflecting the higher confinement ratio and the greater accumulation of strain energy before rupture. In contrast, when steel fibers were incorporated into the UHPC core (UHPFRC), the fibers effectively bridged developing cracks and resisted crack propagation, which significantly reduced spalling and prevented concrete fragmentation. As a result, the FRP-confined UHPFRC specimens exhibited a more controlled failure process, with inclined shear cracks forming within the core but most of the concrete mass remaining inside the FRP jacket. The presence of steel fibers also delayed the onset of hoop rupture, dissipated part of the stored strain energy through progressive fiber pull-out and rupture, and enhanced the post-peak ductility of the specimens. Overall, Wang et al.[89] concluded that steel fiber

TABLE 2 All UHPC mix proportions.

Author	Concrete types	Cement	Water	Fine aggregate	Silica fume	Quartz flour	Super plasticizer	Steel fiber	Other
Guler[87]	UHPC-with fiber	1000	230	628	250	-	32	500	
Deng and Qu[88]	UHPC-with fiber	948	238	1077	238	-	14	79	
Wang et al.[89]	UHPC-without fiber	750	190	1030	225	212	16	0	
	UHPC-with fiber	750	190	1030	225	212	16	191	
Tian et al.[90]	UHPC-with fiber	791	202	930	223	149	12	157	
de Oliveira et al.[91]	UHPC	630	183	900	271	271	50	-	
	UHPC-with heat curing	622	193	889	267	267	50	-	
Liao et al.[92]	UHPC	833	158	916	208	308	33	0	
	UHPC-with fiber							78	
								157	
Ding et al.[93]	UHPC-with fiber	791	202	930	223	149	12	80	
Huang et al.[94]	UHPC-with fiber	674	188	986	169	202	11	196	
Tian et al.[95]	UHPC-with fiber	791	202	930	223	149	12	80	
Wang et al.[96]	UHPC	800	208	960	240	224	40	0	112 Fly ash
	UHPC		240				36	0	
	UHPC-with fiber		208				40	156	
	UHPC-with fiber		240				36	156	
Li et al.[97]	UHPC	968	174	928	155	0	33	0	191 slag
	UHPC-with fiber							156	
Wang et al.[98]	UHPC	850	200	1000	100		11	0	175 Fly ash
	UHPC-with fiber							156	

reinforcement transforms the failure mode from abrupt and explosive to gradual and energy-dissipating, demonstrating a clear improvement in post-peak behavior and structural integrity under axial compression.

In 2022, Ding et al.[93] studied the axial compressive behavior of concrete-filled UHPC tube columns. The circular composite short columns tested consisted of a UHPC tube surrounding an internal concrete core. The UHPC tube had a thickness of 26 mm and a compressive strength of 130 MPa, while the internal concrete core had a strength of 40 MPa. Longitudinal steel bars were combined with spiral carbon FRP (CFRP) or glass FRP (GFRP) stirrups, placed at different spacings within the UHPC tube. The specimens with CFRP and GFRP stirrups failed in a similar pattern. Initially, no significant changes were observed on the UHPC tube surfaces. However, as the axial load increased, cracks gradually formed, leading to failure at the ultimate load. In the specimen with CFRP stirrups spaced at 50 mm, cracks developed at a 45° angle when the load reached 95% of the ultimate load. The specimens failed rapidly, exhibiting brittle failure upon reaching the ultimate load. However, when the CFRP stirrups were spaced at 20 or 35 mm, the failure was more ductile, with a gradual decline in load after peak loading. A similar behavior was observed in the specimens with GFRP stirrups. In the specimen with GFRP stirrups spaced at 50 mm, as the load approached its peak, cracks expanded rapidly, forming a wide main crack. The specimens with stirrup spacings of 20 and 35 mm exhibited more ductile failure behavior similar to those with CFRP stirrups. Overall, closer stirrup spacing (20 and 35 mm) resulted in more ductile failure with slower post-peak load decline, whereas wider spacing (50 mm) led to brittle, rapid load drops.

Li et al.[97] studied the axial compressive behavior of CFRP-partially confined ultra-high-strength concrete (UHSC). They observed that partially confined UHSC fails primarily due to localized concrete crushing and sudden rupture of the CFRP strips, triggered by extensive hoop dilation under axial compression. Distinct crack patterns developed in the confined and unconfined regions: inclined shear cracks appeared within the

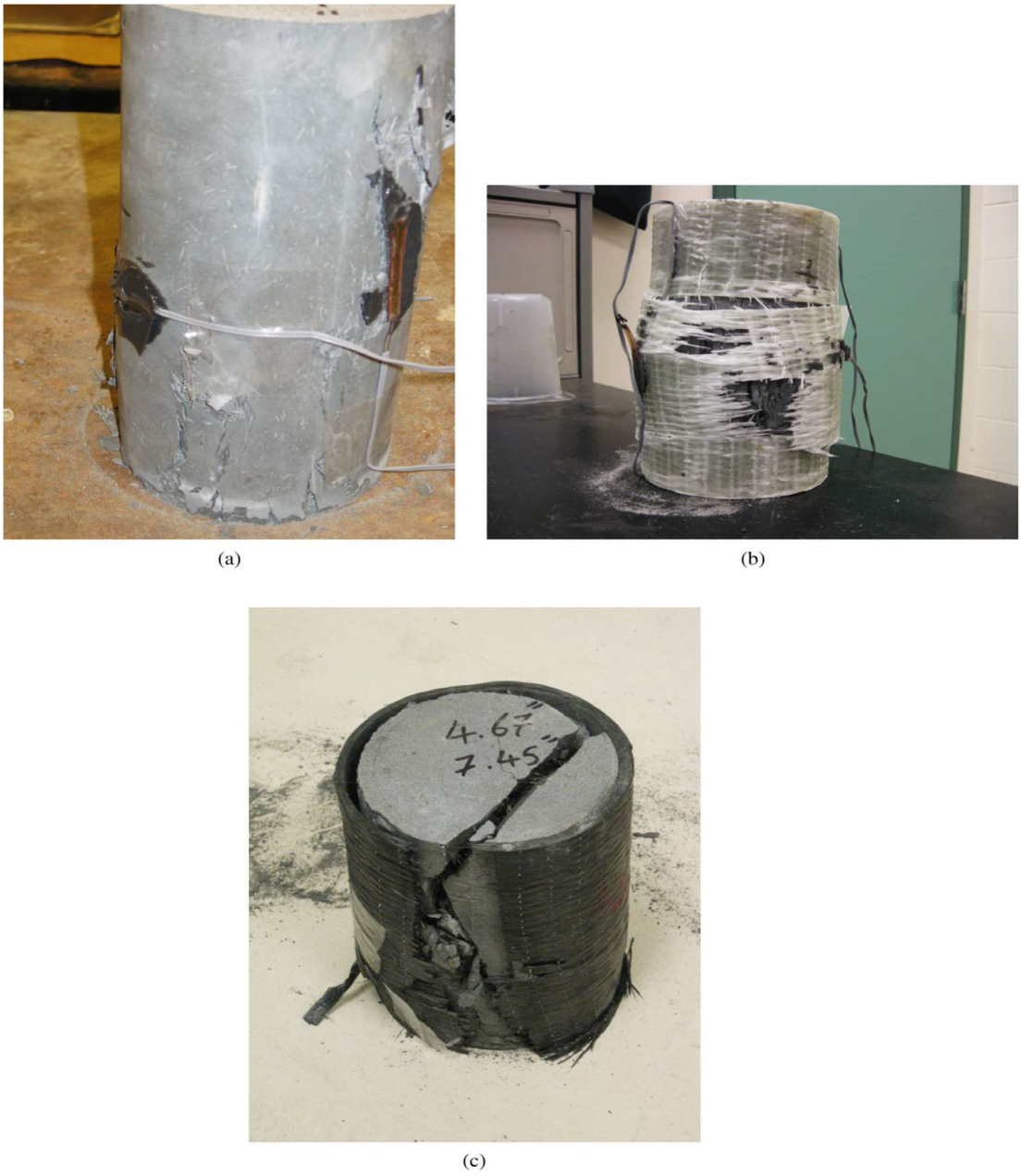

FIGURE 1 Typical failure of (a) unconfined UHPC; (b) UHPC-filled GFRP tube; (c) UHPC-filled CFRP tube.[86]

confined zones, while vertical cracks formed in the unwrapped areas. At the ultimate load, these cracks propagated and merged into a major fracture spanning the entire specimen. Despite the occurrence of sudden strip rupture, the overall structural integrity was maintained because the CFRP strips provided localized stiffness and confinement.

Huang et al.[94] studied the failure modes of unconfined and CFRP-confined UHPC under impact splitting loading. Unconfined UHPC failed in a manner similar to static loading, with a primary crack propagating through the cylinder, and the severity of failure increasing as the strain rate rose. For confined specimens, failure was influenced by both strain rate and CFRP confinement ratio, with strain rate identified as the dominant factor. At low strain rates, CFRP confinement effectively narrowed the main crack and delayed failure, and higher confinement ratios further reduced crack width. At high strain rates, however, the core concrete was crushed into small fragments, obscuring the primary crack pattern, and sudden CFRP rupture released stored energy rapidly. Increasing the number of CFRP layers intensified the damage severity under high strain rates, highlighting that dynamic effects strongly amplify the brittleness of FRP-confined UHPC.

Across the reviewed studies[86–94] consistent trends emerge regarding the failure modes and behavior of FRP-

confined UHPC. CFRP provides the highest peak strength but typically fails through explosive mid-height rupture, resulting in limited post-peak ductility, while GFRP fails more gradually in multi-stage rupture patterns due to its higher tensile strain capacity, leading to improved post-peak energy dissipation. Higher confinement ratios and thicker FRP tubes enhance peak strength but intensify the explosiveness of post-peak failure, whereas partially longitudinal fiber orientations (60°) and closely spaced stirrups or strips promote progressive, ductile failure compared with fully transverse fibers (80°) or wider spacing. Hybrid FRP and the inclusion of steel fibers further delay rupture, control crack propagation, reduce spalling, and stabilize the core, resulting in superior post-peak performance. Overall, the combined effects of FRP type, tube thickness, fiber orientation, confinement ratio, and hybridization directly govern peak strength, ductility, and post-peak behavior, with hybrid and fiber-reinforced systems demonstrating the most stable energy-dissipating performance.

5 | COMPRESSION STRENGTH

Zohrevand and Mirmiran[86] investigated the performance of UHPC specimens confined with various FRP materials under monotonic uniaxial compression. As in Table 3, they found that FRP confinement enhanced the average ultimate strengths of UHPC compared to unconfined UHPC, with the compressive strength of confined concrete improving as the number of FRP layers increases. Additionally, the FRP confinement effectiveness ratios of FRP-confined UHPC were similar to those of FRP-confined high-performance concrete.

Wang et al.[89] studied the performance of FRP-confined UHPC, with or without steel fibers, and compared it with that of FRP-confined NSC and high-strength concrete (HSC). They found that the confinement efficiency of FRP-confined UHPC was lower than that of FRP-confined NSC and HSC, with a sudden reduction in stress observed after the initial peak stress for FRP-confined UHPC.

Guler[87] studied the behavior of cylindrical UHPC samples wrapped with different layers of FRP under axial compression load. He found that FRP wrapping improved the axial strength of UHPC columns; however, the improvement was less than that reported by Zohrevand and Mirmiran.[86] It was found that the axial strength increased with the number of FRP layers. The largest improvement was observed in specimens wrapped with CFRP, as compared to those wrapped with GFRP and AFRP.

In their 2015 study, Deng and Qu[88] compared the behavior of UHPC-filled HFRP tube specimens with unconfined UHPC specimens. They found that UHPC confined within HFRP tubes exhibited greater strength than the unconfined specimens. This enhancement in strength capacity is due to the enhanced lateral confinement provided by the HFRP tubes. It was found that the strength capacity of confined specimens increased depending on the type of hybrid fiber used and the number of fiber sheet layers. Hybrid specimens made of carbon and glass FRP showed the most significant strength improvement and achieved the highest ultimate compressive strength compared to other FRP combinations.

In their 2019 study, Tian et al.[90] examined the axial behavior of FRP-confined UHPC under two different loading conditions: one applied to the cross-section and the other applied only on the UHPC core. They also investigated how the orientation of the FRP fibers and the curing method influenced the compressive performance. It was found that the compressive performance improved when more FRP fibers were oriented in the hoop direction due to enhanced confinement. They found that applying load directly to UHPC cores could prevent the longitudinal buckling of FRP tubes, leading to an increase in the ultimate axial strain. It was noticed that hot-water curing improved the strength of the UHPC core; however, it reduced the strength of the FRP tubes Therefore, it was recommended that hot-water curing should be avoided for UHPC-filled FRP tubes.

Liao et al.[92] found that adding steel fibers to UHPC increased the compressive strength of FRP-confined UHPC by up to 50%, as the steel fibers helped bridge cracks and enhance the material's ability to withstand stress. Ding et al.[93] investigated the use of FRP as spiral straps with different spacing (20, 35, and 50 mm). Their results showed that reducing the spacing of FRP stirrups (i.e., increasing their volumetric ratio) improves concrete confinement, limits lateral expansion, and enhances the axial bearing capacity of the structure by 10%.

Tian et al.[95] investigated the effect of strain gradients on the ultimate strength of FRP-confined concrete columns under axial loading. The axial load was applied at different offsets from the center to create strain gradients across the cross-section. They found that the ultimate strength is affected by both the strain gradient effect and the FRP confinement ratios. The ultimate strength slightly increased under the highest strain gradient when the FRP confinement ratio was high. However, as the confinement ratio decreased, the strength increase became negligible.

The compressive strength of FRP-confined UHPC shows consistent trends across studies. Zohrevand and Mirmiran[86] reported significant strength enhancement with CFRP and GFRP confinement, proportional to the number of FRP layers. Guler[87] observed similar improvements, with CFRP providing the highest gains and GFRP/AFRP more moderate effects. Deng and Qu[88]

TABLE 3 Compression strength.

Author	UHPC strength (kN)	FRP types	FRP thickness (mm)	No. of layers	Compression strength (MPa)
Zohrevand and Mirmiran[86]		N/A	N/A	N/A	188.2
		CFRP	1.02	2	254.1
				4	372.2
		GFRP	1.02	2	188.4
				3	226.6
				4	273.5
				5	298.9
Guler[87]	1250	N/A	N/A	N/A	158.5
		CFRP	0.35	2	168.8
				3	185.5
				4	199.5
				5	235.0
		GFRP	0.35	2	162.9
				3	164.0
				4	179.2
				5	185.7
		AFRP	0.32	2	164.8
				3	177.8
				4	185.0
				5	195.1
Deng and Qu[88]	828	N/A	N/A	N/A	82.8
		A + BFRP	0.53	1	130.4
				2	168.0
				3	208.1
		B + GFRP	0.78	1	122.8
				2	165.2
				3	204.1
		C + BFRP	0.51	1	110.7
				2	162.4
				3	213.2
		C + GFRP	0.60	1	154.0
				2	192.2
				3	260.2
		C2A1G1FRP	0.69	-	128.6
		C2A2G2FRP	1.59	-	201.7
		C2B1G1FRP	1.11	-	139.5
		C2B2G2FRP	1.88	-	195.3
Tian et al.[95]		CFRP 0% steel fiber	0.17	1	109.7
				2	156.2
				3	179.5
		GFRP 0% steel fiber	0.43	6	170.7
				8	201.6

TABLE 3 (Continued)

Author	UHPC strength (kN)	FRP types	FRP thickness (mm)	No. of layers	Compression strength (MPa)
	1400	CFRP 1% steel fiber	0.17	1	130.0
				2	156.7
				3	198.9
		GFRP 1% steel fiber	0.43	6	178.9
				8	216.5
Tian et al.[95]	1250	CFRP	0.167	3	154.4
				4	176.9
				6	227.4

found that HFRP tubes delivered superior strength due to combined lateral restraint, with carbon-glass hybrids performing best. Wang et al.[89] showed that UHPC confinement efficiency is lower than for NSC or HSC, but steel fibers delayed crack propagation and improved peak strength. Tian et al.[90] demonstrated that hoop-oriented fibers increased performance, direct core loading reduced buckling, and hot-water curing enhanced core strength but weakened FRP tubes. Liao et al.[92] reported up to 50% strength gains with steel fibers, while Ding et al.[93] confirmed that closer FRP stirrup spacing improved confinement and axial capacity. Tian et al.[95] noted that high strain gradients only slightly increased strength at high confinement ratios. Overall, compressive strength depends on FRP type, confinement ratio, steel fiber addition, and configuration, with CFRP achieving the highest peaks and HFRP and steel fibers improving post-peak performance.

6 | DYNAMIC STRESS–TIME CURVES

In their 2022 study, Huang et al.[94] explored the dynamic stress–time curves of confined and unconfined UHPC specimens. They found that the stress–time curve for unconfined specimens initially rose and then dropped sharply, with steeper slopes at higher strain rates. As the strain rate increased, the loading time during the ascending phase and the descending phase decreased. In contrast, the confined UHPC showed a different stress–time behavior, particularly in the descending phase. The curve fluctuated during the descending phase, as a result of the confinement effect provided by the FRP jacket. Additionally, it was noted that the ascending phase of the stress–time curve for FRP-confined UHPC lasted longer at low strain rates compared to high strain rates. After reaching the peak load, the FRP jacket became more activated, helping the concrete to withstand splitting stress for a longer period. The capacity of the FRP jacket was increasing as more FRP layers were added. The dynamic splitting tensile strength of FRP-confined UHPC was found to be more dependent on the strain rate, with a stronger effect at higher strain rates.

Su et al.[99] investigated the behavior of ordinary concrete and UHPC under impact loading. They found that the penetration time of the main crack in unconfined UHPC decreases as the impact velocity increases, similar to conventional concrete. However, other studies show that the crack penetration time for UHPC is considerably longer compared to ordinary.[100,101]

Cadoni and Forni[102] and Su et al.[103] suggested that the strain-rate effect in FRP-confined specimens is mainly due to the inherent properties of UHPC. Additionally, they examined the impact of the FRP confinement ratio on the dynamic splitting tensile strength of UHPC across different strain rates. They found that at low to moderate strain rates, the dynamic splitting tensile strength increases with the confinement ratio. However, this effect disappears when the strain rate rises to exceed approximately 10 s^{-1}. This contrasts with previous studies, which indicate that the confinement effect remains effective even at high strain rates in FRP-confined concrete under compressive impact loading.

Huang et al.[94] studied the behaviors of FRP-confined concrete under dynamic compressive and splitting tensile loads. It was found that the behavior under dynamic compressive loads is different from that under splitting tensile loads due to two factors. First, the internal stress distribution varies significantly between the two types of loading. Under splitting loads, the concrete deforms more slowly at low strain rates before the crack fully develops, allowing better confinement from the FRP jacket. However, the concrete fractures quickly at high strain rates, preventing the FRP jacket from providing effective confinement before failure. Second, the expansion of the

FRP jacket is influenced by both concrete cracking and compressive forces along the lateral surface. At high strain rates, lateral deformation becomes significant, which reduces the effectiveness of CFRP confinement.

7 | DYNAMIC STRAIN RATES

Huang et al.[94] investigated the dynamic splitting tensile behavior of CFRP-confined and unconfined specimens. They examined the relationship between striker bar velocity and strain rates. They found that the strain develops in both confined and unconfined specimens at a rate ranging from 2 to 17 s^{-1} depending on the applied velocity of the striker bar.

Su et al.[99] reported similar findings for unconfined UHPC. The strain rate varies between 9 and 18 s^{-1} for unconfined UHPC. The strain rate increased with striker bar velocity. In unconfined specimens, the relationship between strain rate and striker bar velocity followed a linear trend, particularly at higher velocities. The jackets prevented concrete from deforming homogeneously under high velocity impacts, reducing the homogeneity of the specimens, which led to nonlinear behavior of confined concrete. Additionally, the strain rates of the specimens that were confined with FRP were slightly higher compared to those that were not confined when subjected to impact loading at the same striker bar velocity. This finding disagrees with previous research conducted by Bai et al.[30] This discrepancy may be due to differences in impact wave propagation through the wrapped FRP.

8 | STRAIN

Zohrevand and Mirmiran[86] measured the longitudinal and lateral strains in FRP-confined UHPC specimens, reporting a significant increase in ultimate strain (74%–195%) compared to unconfined UHPC, as shown in Table 4. This contrasts with Mandal et al.,[40] who observed lower increases in strain in FRP-confined HSC.

Guler[87] also found that FRP confinement improved the lateral strain of UHPC specimens. Both Zohrevand and Mirmiran[86] and Guler[87] agree that the improvement increases with the number of FRP layers. The confinement was more effective with fewer layers of AFRP and CFRP wraps compared to GFRP-wrapped UHPC columns, where four or five layers provided the greatest improvement.

Zohrevand and Mirmiran,[86] Guler,[87] and de Oliveira et al.[91] observed that strain enhancement due to confinement decreased as ultimate strength increased. Additionally, they agreed with Ozbakkaloglu[104] that a threshold lateral stiffness is required to achieve a significant increase in axial strain, even with confinement.

Wang et al.[89] found that GFRP jackets is better for confining both fiber-reinforced and unreinforced UHPC due to their higher tensile strain capacity compared to CFRP jackets.

Deng and Qu[88] observed that UHPC-filled HFRP tube significantly improved strain capacity compared with unconfined UHPC specimens. The degree of improvement depends on fiber sheet type and number of sheet layers. As the number of layers increases, the thickness of the HFRP tube increases, enhancing the effectiveness of lateral confinement, delaying failure, and improving both compressive strength and ultimate strain. A minimum of four layers was required to achieve this effectiveness. Aramid fiber-reinforced specimens exhibited the highest strain capacity, followed by different GFRP and CFRP hybrid configurations.

Tian et al.[90] found that hot-water curing had opposing effects on UHPC core and outer FRP tubes. It enhanced UHPC core properties but damaged the FRP tubes. The specimen performance could only improve under hot-water curing if the enhancement of the UHPC core outweighed the damage to the FRP tubes. A decrease of up to 31.3% in strain enhancement ratios was observed when hot water was used for curing, suggesting that hot-water curing should be avoided unless the FRP materials are specially treated.

Liao et al.[92] found that adding steel fibers to UHPC significantly increases axial strain by restraining the cracks development in UHPC. The effect of FRP layers was observed through axial-hoop strain curves, showing an initial linear relationship. As concrete dilation increased, the slope of the curve increased, but after reaching an inflection point (a sudden drop in axial stress), the curve becomes linear again, indicating that the cracks gradually grew and the concrete core expanded at nearly a constant rate, with FRP confinement reducing lateral expansion. Ding et al.[93] found that decreasing CFRP stirrup spacing from 50 to 20 mm led to a 90.91% strain increase. Tian et al.[95] found that the ultimate axial strain increases nearly linearly as the strain gradient increases, regardless of the FRP confinement ratio.

The ultimate strain behavior of FRP-confined UHPC shows consistent trends across studies. Zohrevand and Mirmiran[86] reported 74%–195% higher ultimate strains compared with unconfined UHPC, with improvements increasing with the number of CFRP or GFRP layers. Guler[87] similarly found that both axial and lateral strains rise with additional layers, with CFRP and AFRP wraps being more effective at lower layer counts, while GFRP required four to five layers for comparable performance.

TABLE 4 Strain.

Author	UHPC strength (kN)	FRP types	FRP thickness (mm)	No. of layers	Ultimate axial strain
Zohrevand and Mirmiran[86]		N/A	N/A	N/A	0.0039
		CFRP	1.02	2	0.0068
				4	0.0105
		GFRP	1.02	2	0.0040
				3	0.0086
				4	0.0106
				5	0.0115
Guler[87]	1250	N/A	N/A	N/A	0.0109
		CFRP	0.35	2	0.0127
				3	0.0143
				4	0.0174
				5	0.0202
		GFRP	0.35	2	0.0133
				3	0.0158
				4	0.0206
				5	0.0244
		AFRP	0.32	2	0.0127
				3	0.0139
				4	0.0178
				5	0.0211
Deng and Qu[88]	828	N/A	N/A	N/A	0.0030
		A + BFRP	0.53	1	0.0128
				2	0.0181
				3	0.0197
		B + GFRP	0.78	1	0.0111
				2	0.0167
				3	0.0189
		C + BFRP	0.51	1	0.0087
				2	0.0104
				3	0.0129
		C + GFRP	0.60	1	0.0101
				2	0.0147
				3	0.0189
		C2A1G1	0.69	-	0.0103
		C2A2G2	1.59	-	0.0161
		C2B1G1	1.11	-	0.0105
		C2B2G2	1.88	-	0.0150
Tian et al.[95]	1250	CFRP	0.167	3	0.0046
				4	0.0052
				6	0.0062

Deng and Qu[88] demonstrated that hybrid FRP (HFRP) tubes significantly enhance strain capacity, particularly when four or more layers are used, with aramid-based hybrids achieving the highest ductility. Wang et al.[89] showed that GFRP jackets improve strain more effectively than CFRP due to their higher tensile strain

capacity. Tian et al.[90] observed that hot-water curing can reduce strain enhancement by up to 31% because it weakens FRP tubes despite strengthening the UHPC core. Liao et al.[92] found that incorporating steel fibers further increases axial strain by restraining crack development, while Ding et al.[93] reported that reducing CFRP stirrup spacing from 50 to 20 mm nearly doubled strain capacity (≈91% increase). Tian et al.[95] concluded that ultimate axial strain increases almost linearly with higher strain gradients, largely independent of the confinement ratio. Overall, strain capacity depends on FRP type, layer count, hybridization, steel fiber inclusion, and stirrup configuration, with GFRP and hybrid wraps offering superior deformability and steel fibers providing additional ductility.

9 | STRESS–STRAIN BEHAVIOR

Deng and Qu[88] found that the stress–strain behavior of unconfined UHPC is significantly different from that of conventional concrete. The stress–strain curve for unconfined UHPC shows a nearly straight pattern in the ascending phase, whereas conventional concrete displays a nonlinear relationship.

Similarly, Zohrevand and Mirmiran[86] identified a bilinear stress–strain relationship in FRP-confined UHPC specimens, consisting of three distinct regions: an initial phase similar to unconfined UHPC indicating that FRP has not been activated yet, a transition zone where FRP activation begins due to the formation of microcracks and dilation of the UHPC core, and the last stage where FRP is fully activated and effectively resisting progressive dilation of UHPC. In the last stage, the specimen's behavior depends highly on the properties of FRP.

In contrast to Zohrevand and Mirmiran's[86] findings, Wang et al.[89] reported different behaviors. Wang et al.,[89] observed that FRP confinement improves the ductility of UHPC; however, it may lead to a more brittle failure mode compared to normal or high-strength concrete. After reaching the initial peak stress for FRP confined UHPFRC, the stress may drop suddenly, and fluctuations may occur, indicating a loss in concrete's inability to carry load and stating failure. It was observed that the ability of the UHPFRC to recover some of its strength after the initial peak stress depends on the adequacy of the confinement.

In their 2015 study, Deng and Qu[88] examined the stress–strain behavior of UHPC-filled HFRP specimens. They found that the stress–strain curve consists of three different stages: an initial linear phase, a nonlinear transition, and a subsequent linear hardening phase. At the beginning of loading, the stress–strain curve is nearly a straight line, similar to the curve of unconfined UHPC specimens. The stress increases linearly with strain, and the slope of the curve for both confined and unconfined UHPC specimens remains almost constant regardless of the number or type of FRP sheet layers, indicating the HFRP jacket confinement is not yet activated. As loading increases, the behavior of the material changes, and the expansion of the concrete activates the confinement effect of the HFRP jacket, resulting in nonlinear behavior. This stage represents a transition elastic–plastic stage where the stress–strain curve becomes nonlinear. In the final stage, the stress–strain curve becomes nearly a straight line but with a lower gradient than the initial stage, indicating that the HFRP tube provides full confinement, enhancing both the strength and deformation capacity of the specimens. Additionally, it was observed that the increased number of fiber layers contributes to better overall performance under load; specimens wrapped with four or six FRP layers maintained higher stiffness and exhibited greater ultimate strength and strain than those wrapped with two layers.

Tian et al.[90] validated these findings, confirming that the axial stress–strain response of FRP-confined UHPC consists of three stages: linear elastic, transition, and strain hardening. They also found that strength loss may occur in the transition region due to the brittleness of UHPC or weak confinement.

Ozbakkaloglu[104,105] studied the behavior of FRP-confined high-strength concrete and found that it exhibited strain-softening behavior with limited axial strength improvement when confinement is weak but significant strength gains under strong confinement. The confinement threshold separating these behaviors was strongly dependent on unconfined concrete strength, with high-strength concrete requiring a higher level of confinement to reach the same threshold as normal-strength concrete. Similar behavior was observed in square or rectangular columns. Additionally, highly ductile behavior can be achieved when sufficient confinement is provided.

Ozbakkaloglu and Lim[6] found that instrumentation used to measure the axial strain during the compressive tests of FRP-confined cylinders significantly influences axial strain measurements. Strain gauges on the FRP surface and linear variable differential transducers (LVDTs) positioned at midheight show lower strain values than those mounted along the specimen's entire length.

de Oliveira et al.[91] studied the stress–strain behavior of confined concrete. They used strain gauges across the entire specimen length and found that the stress–strain curve has three key regions as shown in Figure 2: an initial quasi-linear zone, a high-curvature transition zone, and a final near-linear zone. The stress–strain curve followed a straight line in the beginning of the loading, indicating an elastic response. As the load increases, the

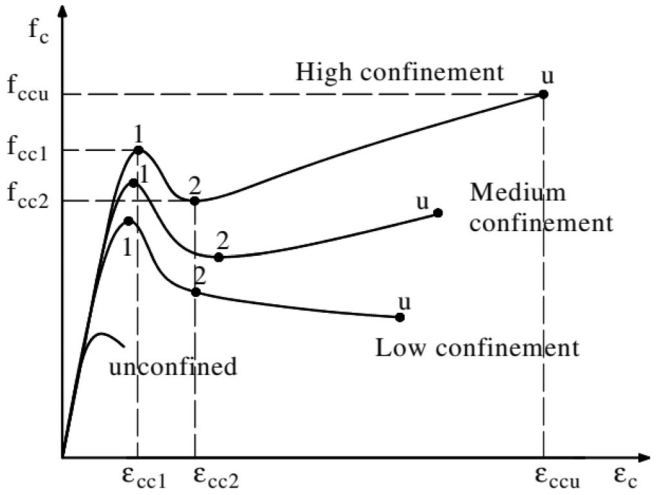

FIGURE 2 Typical stress–strain curves of FRP confined by UHSC.[91]

stress–strain curves followed a nonlinear stage indicating that the confinement effect starts. The confinement level and unconfined concrete strength significantly affect the curvature of the stress–strain curve in this stage. After the second stage, the stress–strain curve returns to be nearly linear with a different slope than the initial phase, indicating the full confinement effect. Regardless of the confinement level, three key points were consistently identified: the beginning of the transitional zone (Point 1) where the nonlinear behavior starts; the end of the transitional zone (Point 2), which was always lower than Point 1; and the end of the final linear branch (Point u), which could be either higher or lower than Point 2, depending on the level of confinement.

Liao et al.[92] studied the axial stress–strain behavior of FRP-confined UHPC. They found that the stress–strain curve typically consists of three stages: an initial linear stage; a transition stage; and a final linear stage. Initial linear stage: at the beginning of loading, the stress–strain curve follows a straight line, meaning that confined UHPC still behaves similarly to unconfined UHPC and the FRP confinement is not yet activated. Transition stage: as the load increases, it starts as cracks begin to develop and UHPC starts to expand, activating the FRP confinement gradually. The final linear segment starts when the FRP confinement is fully activated. It was noticed that the curve slope depends on confinement efficiency.

Additionally, in 2021, Liao et al.[92] investigated the effect of adding steel fiber on the behavior of FRP-confined UHPC columns. Their findings showed that higher steel fiber content extended the duration of the transition stage and slowed the reduction of concrete strength, leading to more gradual stress reduction. The addition of steel fibers also decreased the UHPC brittleness by shifting the crack patterns from sudden splitting and crushing to more gradual widening of the cracks. When the steel fiber content reached 1% volume fraction, the peak stress ratios improved by 20%–50%. The highest improvement (54%) was observed in specimens confined with GFRP. They also compared the stress–strain curves of specimens with different FRP thicknesses but with the same steel fiber content. The results showed that FRP thickness affected the transition and second linear segments of the curves. Specimens with thicker FRP layers showed better crack confinement, leading to a longer transition segment. After the FRP confinement was fully activated, the slope of the second linear segment became more influenced by the thickness of the FRP. This finding supports the findings of Guler[87] who noted that a higher confinement ratio (3–5 layers of wrapping) is required to enhance the strength of UHPC. Increasing FRP thickness can eliminate the stress reduction after the first peak.

Liao et al.[92] also studied how specimen size can affect the behavior of FRP-confined UHPC. They found that FRP-confined UHPC without steel fibers was sensitive to specimen size. Larger specimens exhibited weaker strength due to more structural flaws that become more significant with the increase of the specimens' size. However, the addition of steel fibers helped to reduce the size effect. Adding steel fibers to UHPC bridged the cracks and improved the structural integrity of large specimens, making their stress–strain curves similar to those of smaller ones.

In a similar study, Yoo et al.[106] found that longer steel fibers were more effective in minimizing the specimen size effect. The longer fibers led to a more random orientation and more uniform distribution throughout the specimen.

Mirmiran et al.[107] studied the impact of specimen size on the axial compressive strength of FRP-confined concrete columns. They found that as the height-to-width ratio increased, the axial compressive strength decreased. This is because taller columns are more likely to become unstable and buckle, which leads to a reduction in overall strength.

In 2022, Ding et al.,[93] investigated the axial load–strain behavior of UHPC columns confined by FRP stirrups. The FRP stirrups were placed at various spacings (20, 35, and 50 mm). They found that the load–strain curves exhibited three distinct stages: elastic, elastoplastic, and descending. The elastic stage showed linear behavior. In the elastoplastic stage, the curve slope decreased until reaching the peak load. The descending stage was influenced by stirrup configuration. Wider stirrup spacing led to a rapid load drop due to stirrup fracture, longitudinal bar yielding, and major crack formation, while closer spacing provided better confinement, slowing load reduction.

It was found that FRP stirrups had a minimal effect in the ascending stage. However, stirrup spacing significantly influenced the descending stage, with a slower post-peak decline as spacing decreased. Overall, reducing stirrup spacing enhanced the lateral confinement effect on the internal concrete.

Tian et al.[95] investigated the effect of strain gradients on the stress–strain relationship of UHPC with FRP confinement. Experimental and numerical studies were conducted, and stress–strain curves were then derived using regression analysis. Results showed that the initial stiffness, transition stress, and curvature of the transition region were unaffected by the strain gradient effect; however, the slope of the second ascending branch was most affected. In specimens with a low confinement ratio, the second stiffness decreased by up to 24% under high strain gradients, while specimens with high confinement ratios showed negligible stiffness reduction.

Li et al.[97] investigated the behavior of FRP-partially confined UHPC with and without steel fiber under axial load. They found that the axial stress–strain curve consists of four stages: elastic stage, first ascending stage, rapid reduction stage, and second ascending stage. In the rapid reduction stage, steel fibers significantly improved stress retention and ultimate strength, particularly at high confinement ratios. Stress and strain enhancement ratios are highly influenced by the FRP confinement ratio, especially in specimens with more FRP strips or thicker layers.

Wang et al.[98] studied the behavior of steel tubes confined by UHPC and an outer GFRP layer under concentric compression. They found that the axial load–strain curve comprised four distinct segments: a linear ascending segment, an ascending segment with a decreasing slope, a short descending segment, and a second linear ascending segment.

Huang et al.[108] conducted an experimental study on CFRP-confined UHPC under single and repeated cyclic loading. They found that cyclic axial compression curves exhibit bilinear behavior similar to monotonic stress–strain curves, with slightly higher ultimate strain and stress under cyclic loading. Compared to NSC and HSC, confined UHPC showed a longer initial linear stage and a shorter transition stage.

The stress–strain behavior of FRP-confined UHPC follows a multi-stage pattern influenced by confinement efficiency, material composition, and specimen configuration. Unconfined UHPC exhibits an almost linear ascending curve, unlike the nonlinear response of conventional concrete.[88] Zohrevand and Mirmiran[86] reported a three-stage response: an initial linear phase with inactive FRP, a nonlinear transition as microcracks develop and confinement activates, and a final near-linear phase where FRP resists dilation. Similar observations were confirmed by Deng and Qu[88] and Tian et al.[90] who noted that increasing FRP layers improves stiffness and strain capacity, while hot-water curing may weaken FRP tubes. Wang et al.[89] found that confinement enhances ductility but can still result in sudden post-peak drops when FRP is insufficient. de Oliveira et al.[91] and Ozbakkaloglu[104,105] emphasized that the confinement level and unconfined strength govern the curvature of the transition zone, with weak confinement causing strain-softening. Ozbakkaloglu et al.[6] further showed that axial strain measurements depend on instrumentation and LVDT placement. Liao et al.[92] reported that steel fibers prolong the transition stage, reduce brittleness, and increase peak stress by 20%–50%, while Ding et al.[93] demonstrated that reducing CFRP stirrup spacing slows post-peak decline. Tian et al.[95] noted that strain gradients mainly reduce the slope of the second ascending branch under low confinement. Wang et al.[89] and Wang et al.[98] found that partially confined or multi-layered systems often show four-stage curves, with steel fibers and high confinement ratios improving post-peak retention. Size effects were highlighted by Liao et al.,[92] Yoo et al.,[106] and Mirmiran et al.[107] indicating that larger specimens perform worse unless long steel fibers bridge cracks. Huang et al.[108] further showed that CFRP-confined UHPC under cyclic loading exhibits bilinear curves similar to monotonic behavior but with slightly higher ultimate strain. Overall, FRP-confined UHPC develops three to four-stage stress–strain curves controlled by FRP type, layer count, hybridization, steel fiber content, confinement ratio, and specimen geometry, with proper confinement and fiber inclusion promoting ductile, energy-dissipating performance.

10 | ENERGY ABSORPTION AND DUCTILITY

The energy-dissipating performance and ductility of FRP-confined UHPC are primarily governed by the interaction between confinement effectiveness, material composition, and structural configuration. As shown in Table 5, FRP confinement significantly improves the ductility of UHPC and UHPFRC compared to their unconfined counterparts; however, the dense microstructure and limited internal crack-bridging capacity of UHPC make it inherently less ductile than FRP-confined normal-strength or high-strength concrete.[89] This highlights that lateral FRP confinement alone cannot fully overcome the intrinsic brittleness of UHPC.

Early studies by Deng and Qu[88] demonstrated that HFRP tubes, combining the high stiffness of CFRP with the greater strain capacity of GFRP or AFRP, provide a more balanced and effective confinement system than

TABLE 5 Comparative summary of experimental studies on FRP-confined UHPC columns.

Study	Specimen type/ geometry	FRP type and confinement	No. of layers/ spacing	Steel fiber dosage and orientation	Failure mode	Confinement effectiveness
Deng and Qu[88]	UHPC-filled hybrid FRP tube	HFRP (hybrid GFRP + CFRP/ AFRP)	Multiple layers (thicker tubes)	-	FRP rupture after concrete crushing	Enhanced ductility; delayed failure; improved compressive strength and ultimate strain
Wang et al.[89]	UHPFRC and plain UHPC cylinders	CFRP and GFRP full confinement	1–9 layers	0%–2%; random 3D	Explosive rupture (plain UHPC); controlled with fibers	Steel fibers prevented spalling; CFRP enhanced strength; GFRP improved ductility
Tian et al.[90]	UHPC cylinders with varying fiber orientation	GFRP full confinement (60° and 80°)	2–5 layers	1.5%–2%; hoop/axial	Mid-height FRP rupture; progressive at 60°	Hoop-oriented fibers and hot curing improved strength; high ductility under optimized orientation
de Oliveira et al.[91]	Small UHPC cylinders (50 × 100 mm)	CFRP and GFRP full confinement	1–4 layers	-	FRP rupture with vertical cracks	Three-stage stress–strain; hot curing enhanced UHPC but slightly weakened FRP tubes
Liao et al.[92]	UHPC circular columns (50 and 100 mm diameters)	CFRP and GFRP full confinement	1–8 layers	0%–2%; random 3D	FRP rupture	Steel fibers increased energy absorption (up to 50%); CFRP > GFRP in strength and stiffness
Ding et al.[93]	UHPC columns with FRP spiral straps	CFRP and GFRP straps	20, 35, 50 mm spacing	0%–2%; random 3D	Crushing + localized FRP rupture	Closer spacing (20 mm) doubled ductility; delayed failure and slower post-peak decay
Huang et al.[94]	UHPC under dynamic impact (SHPB)	CFRP full confinement	1–3 layers	1%–2%; random	High-rate explosive rupture	CFRP reduced crack width at low strain rates; high rates caused core fragmentation
Tian et al.[95]	UHPC columns under strain gradient loading	CFRP and GFRP full confinement	1–8 layers	1.5%; random	FRP rupture at high strain gradient	Strength slightly increased at high gradients for high confinement ratios
Wang et al.[96]	UHPC cylinders (100 × 200 and 150 × 300 mm)	CFRP and GFRP full confinement	2–5 layers	1.5%; random	Mid-height rupture	Confinement improved strength; GFRP increased ductility
Li et al.[97]	Partially CFRP-confined UHPC columns	CFRP partial wraps	Strip spacing 20–60 cm	1.5%; random	Localized buckling and FRP rupture	Limited strain enhancement; accurate strength prediction
Wang et al.[98]	Steel tube + UHPC core + GFRP outer confinement	GFRP full wrapping over steel tube	4–6 layers	1.5%; random	Localized FRP rupture with steel tube yielding	Four-stage response; combined steel and FRP confinement improved post-peak energy dissipation

single-type FRP. HFRP confinement delays failure, enhances ultimate strain, and increases strain-energy absorption, with ductility gains rising proportionally to the number of FRP layers. Thicker hybrid tubes generate stronger lateral restraint and greater post-peak energy dissipation, while steel fibers further stabilize the UHPC core by bridging cracks and reducing explosive spalling. Wang and Wu[89] confirmed that although CFRP and GFRP jackets improve ductility, plain FRP-confined UHPC still fails in a brittle manner, whereas the inclusion of steel fibers transforms the failure process into a more controlled, energy-dissipating response.

Further investigations by Liao et al.[92] and Tian et al.[95] emphasized that ductility enhancement is strongly linked to strain-energy absorption, with CFRP providing superior energy dissipation due to its higher elastic modulus, which allows confining pressure to mobilize more efficiently as UHPC dilates. In contrast, GFRP and hybrid wraps exhibit superior deformability, which is particularly beneficial in sustaining post-peak ductility. Liao,

Yang[92] also demonstrated that incorporating steel fibers can increase ductility by up to 50%, prolonging the transition phase of the stress–strain curve and delaying sudden load drops.

Geometric and configuration optimizations also play a critical role in enhancing ductility. Ding et al.[93] showed that reducing FRP spiral or stirrup spacing from 50 to 20 mm significantly increases post-peak ductility by providing stronger lateral restraint, delaying crack localization, and slowing the rate of stress decline, which is crucial for seismic and dynamic applications. Huang et al.[94] found that under high strain rate or impact loading, CFRP confinement effectively delays fragmentation and enhances energy absorption, although failure severity increases with strain rate. Li et al.[97] and Wang et al.[98] further demonstrated that partial confinement and hybrid systems, such as steel-tube-and-GFRP configurations, can maintain structural integrity and improve energy dissipation, though maximum energy absorption occurs with full or hybrid FRP confinement.

Importantly, the effectiveness of these configurations is strongly influenced by steel fiber dosage and orientation within the UHPC core. Low fiber dosages (<1%) primarily delay initial crack formation, whereas higher dosages (≈1.5%–2%) promote multiple fine cracks, suppress spalling, and enhance energy absorption by up to 50%.[89,92] Moreover, fiber orientation contributes to strain development: fibers randomly distributed in 3D provide uniform crack bridging, while preferential alignment along the hoop or axial directions enhances localized crack control under FRP confinement. When combined with optimized spiral spacing and hybrid FRP jackets, adequately dosed steel fibers transform brittle UHPC failure into a gradual, multi-stage, energy-dissipating response suitable for static, cyclic, and high-strain-rate applications.

The energy-dissipating performance and ductility of FRP-confined UHPC are governed by confinement ratio, FRP type, fiber orientation, tube thickness, hybridization, steel fiber addition, and geometric configuration, as summarized in Table 5. FRP confinement enhances ductility and energy absorption compared to unconfined UHPC, though UHPC remains less ductile than FRP-confined normal or high-strength concrete due to its dense microstructure and limited crack-bridging capacity.[89] CFRP provides the highest peak strength but often fails abruptly, whereas GFRP offers lower peak strength but superior post-peak ductility.[89,90,92] HFRP systems balance stiffness and deformability, delaying failure and improving ultimate strain and energy dissipation.[88] Fiber orientation influences ductility; hoop-oriented GFRP wraps at 60° delay mid-height rupture more effectively than at 80°.[90] Tube thickness and number of layers increase confinement, extending post-peak response,[88,92] while steel fibers stabilize the core, reduce spalling, and increase energy absorption by up to 50%.[89,92] Geometric optimization, such as reducing spiral or strap spacing from 50 to 20 mm, nearly doubles ductility and slows stress decay.[93] Under high-strain-rate loading, CFRP delays fragmentation,[94] and hybrid steel-tube + GFRP systems show four-stage responses with superior post-peak energy dissipation.[98]

The role of steel fibers in FRP-UHPC systems depends strongly on dosage and orientation. Low dosages (<1%) mainly delay initial crack formation, while higher dosages (≈1.5%–2%) promote multiple fine cracks, enhancing post-peak energy dissipation and reducing spalling.[89,92] Random three-dimensional distributions provide uniform crack bridging, whereas preferential hoop or axial alignment improves localized crack control and strain development under FRP confinement. When combined with optimized spiral spacing, adequate FRP layers, and hybrid FRP jackets, properly dosed steel fibers enable UHPC to transition from brittle, single-stage failure to a gradual, multi-stage, energy-dissipating response suitable for static, cyclic, and dynamic conditions. Table 5 confirms that maximum ductility and energy absorption are achieved with high confinement ratios, hybrid FRP, favorable fiber orientation, sufficient tube thickness, closely spaced spirals, and steel-fiber-reinforced UHPC cores.

11 | MODELING

Several models have been developed to predict the axial compressive behavior of UHPC columns confined with different types of FRP sheets. Zohrevand and Mirmiran[86] adapted two widely used FRP-confined NSC models, namely those developed by Samaan et al.[37] and Lam and Teng,[39] to estimate the stress–strain behavior of FRP-confined UHPC. While these models provided a foundational framework, their assumptions regarding dilation capacity and ductile post-peak behavior are not fully applicable to UHPC. UHPC exhibits a denser matrix and reduced lateral expansion compared to NSC, which affects how confinement develops.

Guler[87] proposed an analytical model for predicting the ultimate strength of FRP-confined UHPC based on experimental testing. Although this model improved strength predictions over earlier approaches, it consistently underestimated axial stress values when compared to later experimental data. Wang and Wu[89] evaluated both the Zohrevand and Mirmiran[86] and Guler[87] models. Their findings indicated that Zohrevand and Mirmiran's model showed more than 40% error in predicting compressive strength and ultimate strain, while Guler's model performed better but still lacked general accuracy. These discrepancies were mainly due to limited calibration datasets and the complexity of UHPC behavior.

To improve strain prediction and post-peak response, Liao et al.[92] developed two models. The first model provided reasonable predictions for characteristic stresses and showed good agreement with experimental data during the FRP activation phase. However, it underperformed in estimating ultimate strain, particularly at higher confinement levels or with steel fiber inclusion. This limitation highlighted the challenges in accurately simulating the transition and softening phases of UHPC under confinement.

Wang et al.[98] evaluated a wide range of stress–strain models and confirmed that those developed for NSC and HSC, such as Vincent and Ozbakkaloglu[109] and Sadeghian et al.[110] were not suitable for UHPC and UHPFRC. They found that the models proposed by Zohrevand and Mirmiran,[86] Lam and Teng,[39] and Liao et al.[92] could estimate stress enhancement ratios with moderate accuracy, but consistently failed to capture strain development across different confinement types and specimen geometries.

Pan et al.[76] conducted a detailed experimental investigation on UHPC-filled FRP tubes using three confinement types: CFRP, GFRP, and BFRP, combined with both plain UHPC and fiber-reinforced UHPC cores. Their results demonstrated that CFRP offered the highest confinement efficiency, while GFRP and BFRP showed relatively lower improvements in strength and ductility. The study provided full stress–strain curves, captured confinement effects under various configurations, and emphasized the importance of fiber type and core composition on post-peak behavior. This robust dataset helps bridge existing gaps in current model calibration, especially under diverse confinement scenarios.

Huang et al.[108] introduced a design-oriented model for CFRP-confined UHPC under cyclic axial loading. This model incorporated cyclic effects and provided a more accurate prediction of stress and strain paths under repeated compression. Ding et al.[93] developed a validated numerical model based on experimental data for CFRP-confined UHPC. Their model successfully predicted peak load and initial stiffness by accounting for the compressive strength of the core and the thickness of the confinement tube.

Li et al.[97] proposed a model focused on partially confined UHPC columns wrapped with CFRP strips. Their formulation showed good agreement with experimental results, particularly in cases involving varying strip spacing. This study addressed a major limitation in prior models, which typically assume full circumferential confinement. However, the proposed model remains limited to static loading conditions and cannot be directly applied to dynamic or cyclic cases. Zeng et al.[111] extended the understanding of partially confined UHPC by conducting systematic experimental and numerical investigations on CFRP-wrapped circular columns. Their results confirmed that varying the strip spacing significantly affects both peak strength and ductility. The proposed finite element model incorporated detailed bond behavior and stress transfer mechanisms between the CFRP and UHPC, yielding high accuracy in predicting stress–strain responses under partial confinement. This study offers an important advancement over previous models by enabling reliable performance evaluation under discontinuous or non-uniform confinement conditions. Liao et al.[112] conducted a comprehensive experimental and numerical investigation on UHPC columns confined with CFRP under both fully and partially wrapped conditions. Their study evaluated the effects of confinement ratio and configuration on peak stress, strain development, and post-peak behavior. A validated finite element model was developed using explicitly measured dilation rates and confinement stiffness, showing excellent agreement with test results across different CFRP layouts. The model also captured confinement activation and strain hardening mechanisms with high precision, supporting its use in design applications for both continuous and discontinuous confinement scenarios.

A dynamic prediction model was also introduced for CFRP-confined UHPC based on a logarithmic relationship between strain rate and the dynamic increase factor. While this model provided a general estimation of dynamic performance, it showed discrepancies when compared to test results, especially at high strain rates. The deviation was attributed to limited dynamic testing data and the complex interaction between the FRP confinement and inertial effects during impact.

As illustrated in Figure 3 and confirmed by the reviewed studies, most current models have notable limitations. Early models, such as those by Zohrevand and Mirmiran[86] and Vincent and Ozbakkaloglu,[109] tend to underestimate both compressive strength and ultimate strain due to their simplified representation of UHPC behavior. Additionally, few models are capable of handling partial confinement conditions or strain-rate sensitivity. More recent models, including those developed by Liao et al.,[92] Ding et al.,[93] Huang et al.,[108] and Li et al.[97] offer improved predictive performance. These models capture confinement activation, cyclic effects, and partial wrapping, but still face challenges in generalizing across different confinement ratios, fiber dosages, and loading conditions. A recent contribution by Wang et al.[113] introduced a design-oriented constitutive model specifically developed for FRP-confined UHPC circular columns. The model was calibrated using an extensive set of experimental stress–strain data and incorporates key parameters such as confinement stiffness, energy dissipation capacity, and post-peak ductility. It effectively addresses several limitations of earlier models, particularly regarding strain prediction and

Number	Model	Scope	Axial stress at ultimate condition f_{cu}	Ultimate strain ε_{cu}
1	Teng et al. (2009) [39]	NSC	$\frac{f_{cu}}{f_{co}} = 1 + 3.5(\rho_k - 0.001)\rho_r$, $\rho_r = \frac{\varepsilon_{h,rup}}{\varepsilon_{co}} (\rho_k \geq 0.01)$	$\frac{\varepsilon_{cu}}{\varepsilon_{co}} = 1.75 + 6.5\rho_k^{0.8}\rho_r^{1.45}$
2	Lim and Ozbakkaloglu (2014) [41]	HSC	$f_{cu} = c_1 f'_{co} + 3.2\left(f_{l,a} - f_{lo}\right)$, $K_l = 2E_{frp}t_{frp}/D, K_{lo} = f'^{1.65}_{co}$, If $K_l \geq K_{lo}, c_1 = 1 + 0.0058K_l/f'_{co}$, $f_{lo} = K_l(0.43 + 0.009K_l/f'_{co})\varepsilon_{co}$; If $K_l < K_{lo}, c_1 = \left(K_l/f'^{1.6}_{co}\right)^{0.2}$, $f_{lo} = 24K_l(f'_{co}/K_l^{1.6})^{0.4}\varepsilon_{co}$.	$\varepsilon_{cu} = c_2\varepsilon_{co} + 0.27\left(\frac{K_l}{f'_{co}}\right)^{0.9}\varepsilon_{h,rup}^{1.35}$, $c_2 = 2 - \left(\frac{f'_{co} - 20}{100}\right)$ and $c_2 \geq 1$.
3	Zohrevand and Mirmiran (2013) [45]	UHPFRC	$\frac{f_{cu}}{f_{co}} = 1 + 0.107\frac{f_{l,a}^2}{f'_{co}}$	$\frac{\varepsilon_{cu}}{\varepsilon_{co}} = \frac{f'_{cu} - f_o}{E_2\varepsilon_{co}}$, $f_o = 0.7862f'_{cu} + 0.455f_{l,a}$, $E_2 = 1350.76f'^{0.2}_{co} + 5.675\frac{E_{frp}t_{frp}}{D}$.
4	Zohrevand and Mirmiran (2013) [45]	UHPFRC	$\frac{f_{cu}}{f_{co}} = 1 + 3.2519\frac{f_{l,a}}{f'_{co}}$	$\frac{\varepsilon_{cu}}{\varepsilon_{co}} = 1.1075 + 8.836\left(\frac{E_{frp}t_{frp}}{E_cD}\right)\left(\frac{\varepsilon_{h,rup}}{\varepsilon_{co}}\right)^2$
5	Guler (2014) [23]	UHPFRC	$\frac{f_{cu}}{f_{co}} = 1 + 0.55\frac{f_{l,a}}{f'_{co}}$	Not available
6	Lam et al. (2021) [25]	UHPFRC	$\frac{f_{cu}}{f_{co}} = 1 + 2.8\frac{f_{l,a}}{f'_{co}}$	$\frac{\varepsilon_{cu}}{\varepsilon_{co}} = 1 + 8.3\frac{f_{l,a}}{f'_{co}}\left(\frac{\varepsilon_{h,rup}}{\varepsilon_{co}}\right)^{0.45}$
7	Liao et al. (2022) [46]	UHPC /UHPFRC	For CFRP confinement, if $V_{sf} = 0\%$, $\rho_k < 0.075$; if $V_{sf} = 2\%$, $\rho_k < 0.036$. For GFRP confinement, if $V_{sf} = 0\%$, $\rho_k < 0.083$; if $V_{sf} = 2\%$, $\rho_k < 0.06$. $\frac{f_{c1}}{f_{co}} = 1 + 0.254\left(\frac{f_{l,a}}{f'_{co}}\right)^{0.6}\left(\frac{\varepsilon_{h,rup}}{\varepsilon_{co}}\right)$, $\frac{f_{c2}}{f_{co}} = 0.827 + 1.224\left(\frac{f_{l,a}}{f'_{co}}\right)^{0.8}\left(\frac{\varepsilon_{h,rup}}{\varepsilon_{co}}\right)^{0.2}$, $\frac{f_{cu}}{f_{co}} = 0.56 + 2.35\left(\frac{f_{l,a}}{f'_{co}}\right)^{0.6}\left(\frac{\varepsilon_{h,rup}}{\varepsilon_{co}}\right)^{0.1}$.	$\frac{\varepsilon_{c1}}{\varepsilon_{co}} = 1 + 1.922\left(\frac{f_{l,a}}{f'_{co}}\right)^{0.8}\left(\frac{\varepsilon_{h,rup}}{\varepsilon_{co}}\right)^{0.1}$, $\frac{\varepsilon_{c2}}{\varepsilon_{co}} = 1.153 + 0.359\left(\frac{f_{l,a}}{f'_{co}}\right)^{0.1}\left(\frac{\varepsilon_{h,rup}}{\varepsilon_{co}}\right)^{0.8}$, $\frac{\varepsilon_{cu}}{\varepsilon_{co}} = 1.263 + 1.809\left(\frac{f_{l,a}}{f'_{co}}\right)^{0.1}\left(\frac{\varepsilon_{h,rup}}{\varepsilon_{co}}\right)^{0.7}$.
			For CFRP confinement, if $V_{sf} = 0\%$, $\rho_k \geq 0.075$; if $V_{sf} = 2\%$, $\rho_k \geq 0.036$. For GFRP confinement, if $V_{sf} = 0\%$, $\rho_k \geq 0.083$; if $V_{sf} = 2\%$, $\rho_k \geq 0.06$. $\frac{f_{cu}}{f_{co}} = 1 + 0.606\left(\frac{f_{l,a}}{f'_{co}}\right)^{0.6}\left(\frac{\varepsilon_{h,rup}}{\varepsilon_{co}}\right)^{0.7}$	$\frac{\varepsilon_{cu}}{\varepsilon_{co}} = 1 + 0.595\left(\frac{f_{l,a}}{f'_{co}}\right)^{0.1}\left(\frac{\varepsilon_{h,rup}}{\varepsilon_{co}}\right)^{1.45}$

FIGURE 3 Models of ultimate strength of UHPC columns confined with FRP.[93]

the accurate representation of the transition zone between elastic and plastic behavior. Compared to previous approaches, this model demonstrated improved accuracy across various confinement levels and offers enhanced reliability for the structural design and performance assessment of FRP-confined UHPC columns under static loading conditions. Zeng et al.[111] developed and experimentally validated a nonlinear finite element model to simulate the axial compressive behavior of UHPC confined with FRP tubes. The model accurately captured the entire stress–strain response, including the peak strength, post-peak softening, and strain development. Their findings highlighted the significant influence of confinement stiffness and core dilation behavior on the ultimate performance. The model also demonstrated the importance of incorporating appropriate dilation parameters and bond-slip conditions to improve prediction accuracy across different fiber configurations and confinement levels.

To improve the accuracy and practical applicability of future modeling approaches for FRP-confined UHPC, several key advancements are necessary. First, models should be calibrated using comprehensive experimental datasets that encompass a wide range of FRP types, wrapping configurations, confinement ratios, and concrete strengths. Second, the influence of steel fibers, particularly their effects on post-peak softening, crack bridging, and strain development, should be explicitly incorporated into the modeling framework. Third, validated models are needed to account for complex structural conditions, including partial confinement, eccentric loading, and strain gradient effects.

Finally, integrating strain rate-dependent behavior is essential to accurately simulate dynamic and impact loading scenarios. Zeng et al.[114] further advanced this field by developing a modified design-oriented stress–strain model for CFRP-confined UHPC, calibrated against a wide range of experimental datasets and validated through parametric analysis. Their model incorporated key confinement parameters such as effective lateral stress and dilation behavior, and it showed improved prediction accuracy across various confinement ratios and concrete strengths.

Addressing these aspects will support the development of more reliable and design-oriented predictive models for FRP-confined UHPC columns under both static and dynamic conditions.

12 | CONCLUSIONS

Based on the extensive review and discussion of the behavior of FRP reinforced UHPC tubes, the following conclusions can be drawn:

- UHPC generally fails under axial compressive load through lateral tensile expansion. The ultimate strength capacities of the UHPC columns can be significantly enhanced by FRP confinement, and this enhancement increases with higher confinement levels.
- The ultimate strain capacities of the UHPC columns can be significantly enhanced by FRP confinement, and this enhancement increases with higher confinement levels.
- For the same level of FRP confinement, the highest increase in ultimate strength is observed in CFRP-confined UHPC columns, as CFRP has higher stiffness compared to other FRP types such as AFRP and GFRP.
- The highest increase in ultimate strain is observed in GFRP-confined UHPC columns, as GFRP exhibits more ductile properties such as a lower tensile elastic modulus and a higher elongation capacity, compared with AFRP and CFRP sheets.
- FRP confinement significantly enhances ductility by increasing strain energy absorption. Additionally, CFRP confinement shows better energy absorption capacity than GFRP confinement due to its higher elastic modulus.
- Several models were developed, providing reasonable predictions of the ultimate strength of UHPC columns confined with different types of FRP sheets and showing good agreement with experimental results.

13 | FUTURE WORK

It is clear from previous studies that there is a gap that was not covered by previous studies, which can be mentioned as follows:

- Dynamic behavior of UHPC confined with GFRP and AFRP.
- Effect of steel fiber on the dynamic behavior of UHPC confined with GFRP and AFRP.
- Effect of strain gradient on the tube of UHPC confined by GFRP and AFRP and its stress–strain relationship.
- Effect of strain gradient on the stress–strain relationship of UHPC with different percentages of steel fiber tube confined by CFRP, GFRP, and AFRP.
- Behavior and failure mode of GFRP and AFRP partially confined UHPC.
- Dynamic behavior and failure mode of CFRP, GFRP, and AFRP partially confined UHPC.

CONFLICT OF INTEREST STATEMENT

The authors declare no conflicts of interest.

DATA AVAILABILITY STATEMENT

The data that support the findings of this study are available on request from the corresponding author. The data are not publicly available due to privacy or ethical restrictions.

ORCID

Mustafa Maher Al-Tayeb https://orcid.org/0000-0001-9451-3277
Bassam A. Tayeh https://orcid.org/0000-0002-2941-3402
Nurdeen M. Altwair https://orcid.org/0009-0003-2076-0832
Abdullah M. Zeyad https://orcid.org/0000-0003-0023-8249

REFERENCES

1. Liao J, Zeng JJ, Bai YL, Zhang L. Bond strength of GFRP bars to high strength and ultra-high strength fiber reinforced seawater sea-sand concrete (SSC). Compos Struct. 2022;281:115013.
2. Wu Y-F, Jiang C. Effect of load eccentricity on the stress–strain relationship of FRP-confined concrete columns. Compos Struct. 2013;98:228–41.
3. Zeng J, Lin G, Teng JG, Li LJ. Behavior of large-scale FRP-confined rectangular RC columns under axial compression. Eng Struct. 2018;174:629–45.
4. Zhou Y, Zheng Y, Sui L, Xing F, Hu J, Li P. Behavior and modeling of FRP-confined ultra-lightweight cement composites under monotonic axial compression. Compos Part B Eng. 2019;162:289–302.
5. Wei Y-Y, Wu Y-F. Unified stress–strain model of concrete for FRP-confined columns. Construct Build Mater. 2012;26(1):381–92.
6. Ozbakkaloglu T, Lim JC, Vincent T. FRP-confined concrete in circular sections: review and assessment of stress–strain models. Eng Struct. 2013;49:1068–88.
7. Cao Y-G, Jiang C, Wu Y-F. Cross-sectional unification on the stress–strain model of concrete subjected to high passive confinement by fiber-reinforced polymer. Polymers. 2016;8(5):186.
8. Wei Y, Wu G, Li G. Performance of circular concrete-filled fiber-reinforced polymer–steel composite tube columns under axial compression. J Reinf Plast Compos. 2014;33(20):1911–28.

9. Jiang C, Wu Y-F, Jiang J-F. Effect of aggregate size on stress–strain behavior of concrete confined by fiber composites. Compos Struct. 2017;168:851–62.
10. Wang J, Feng P, Hao T, Yue Q. Axial compressive behavior of seawater coral aggregate concrete-filled FRP tubes. Construct Build Mater. 2017;147:272–85.
11. Pan Y, Cao SY, Jing DH, Zhao SC. Experimental research on axially loaded circular concrete columns confined by CFRP under preload. Adv Mater Res. 2011;255:694–8.
12. Yu T, Zhang S, Huang L, Chan C. Compressive behavior of hybrid double-skin tubular columns with a large rupture strain FRP tube. Compos Struct. 2017;171:10–8.
13. Wang W, Sheikh MN, Hadi MNS, Gao D, Chen G. Behaviour of concrete-encased concrete-filled FRP tube (CCFT) columns under axial compression. Eng Struct. 2017;147:256–68.
14. Jameel MT, Sheikh MN, Hadi MN. Behaviour of circularized and FRP wrapped hollow concrete specimens under axial compressive load. Compos Struct. 2017;171:538–48.
15. Hadi MN, Wang W, Sheikh MN. Axial compressive behaviour of GFRP tube reinforced concrete columns. Construct Build Mater. 2015;81:198–207.
16. Wang W, Sheikh MN, Hadi MN. Behaviour of perforated GFRP tubes under axial compression. Thin-Walled Struct. 2015;95:88–100.
17. Wang W, Sheikh MN, Hadi MN. Axial compressive behaviour of concrete confined with polymer grid. Mater Struct. 2016;49:3893–908.
18. Wang W, Sheikh MN, Hadi MN. Experimental study on FRP tube reinforced concrete columns under different loading conditions. J Compos Construct. 2016;20(5):4016034.
19. Lim JC, Ozbakkaloglu T. Influence of silica fume on stress–strain behavior of FRP-confined HSC. Construct Build Mater. 2014;63:11–24.
20. Ozbakkaloglu T, Vincent T. Axial compressive behavior of circular high-strength concrete-filled FRP tubes. J Compos Construct. 2014;18(2):4013037.
21. Cao S, Hou X, Rong Q, Li G. Dynamic splitting tensile test of hybrid-fiber-reinforced reactive powder concrete. Emerg Mater Res. 2017;7(1):52–7.
22. Cao Y, Wu Y-F, Jiang C. Stress–strain relationship of FRP confined concrete columns under combined axial load and bending moment. Compos Part B Eng. 2018;134:207–17.
23. Chen D, Liu F, Yang F, Jing L, Feng W, Lv J, et al. Dynamic compressive and splitting tensile response of unsaturated polyester polymer concrete material at different curing ages. Construct Build Mater. 2018;177:477–98.
24. Zeng J-J, Chen SP, Zhuge Y, Gao WY, Duan ZJ, Guo YC. Three-dimensional finite element modeling and theoretical analysis of concrete confined with FRP rings. Eng Struct. 2021;234:111966.
25. Ferrotto M, Fischer O, Cavaleri L. A strategy for the finite element modeling of FRP-confined concrete columns subjected to preload. Eng Struct. 2018;173:1054–67.
26. Ferrotto MF, Fischer O, Niedermeier R. Experimental investigation on the compressive behavior of short-term preloaded carbon fiber reinforced polymer-confined concrete columns. Struct Concr. 2018;19(4):988–1001.
27. Zhou J-K, Lin WK, Guo SX, Zeng JJ, Bai YL. Behavior of FRP-confined FRP spiral reinforced concrete square columns (FCFRCs) under axial compression. J Build Eng. 2022;45:103452.
28. Ren F, Liang YW, Ho JCM, Lai MH. Behaviour of FRP tube-concrete-encased steel composite columns. Compos Struct. 2020;241:112139.
29. Song J, Gao WY, Ouyang LJ, Zeng JJ, Yang J, Liu WD. Compressive behavior of heat-damaged square concrete prisms confined with basalt fiber-reinforced polymer jackets. Eng Struct. 2021;242:112504.
30. Bai Y-L, Yan ZW, Ozbakkaloglu T, Gao WY, Zeng JJ. Mechanical behavior of large-rupture-strain (LRS) polyethylene naphthalene fiber bundles at different strain rates and temperatures. Construct Build Mater. 2021;297:123786.
31. Wang W, Sheikh MN, al-Baali AQ, Hadi MNS. Compressive behaviour of partially FRP confined concrete: experimental observations and assessment of the stress–strain models. Construct Build Mater. 2018;192:785–97.
32. Xiao Q, Teng J, Yu T. Behavior and modeling of confined high-strength concrete. J Compos Construct. 2010;14(3):249–59.
33. Li P, Wu Y-F, Gravina R. Cyclic response of FRP-confined concrete with post-peak strain softening behavior. Construct Build Mater. 2016;123:814–28.
34. Tang Z, Li W, Tam VWY, Yan L. Mechanical behaviors of CFRP-confined sustainable geopolymeric recycled aggregate concrete under both static and cyclic compressions. Compos Struct. 2020;252:112750.
35. Lai M, Liang YW, Wang Q, Ren FM, Chen MT, Ho JCM. A stress-path dependent stress–strain model for FRP-confined concrete. Eng Struct. 2020;203:109824.
36. Wu G, Wu Z, Lü Z. Design-oriented stress–strain model for concrete prisms confined with FRP composites. Construct Build Mater. 2007;21(5):1107–21.
37. Samaan M, Mirmiran A, Shahawy M. Model of concrete confined by fiber composites. J Struct Eng. 1998;124(9):1025–31.
38. Teng J, Jiang T, Lam L, Luo YZ. Refinement of a design-oriented stress–strain model for FRP-confined concrete. J Compos Construct. 2009;13(4):269–78.
39. Lam L, Teng JG. Design-oriented stress–strain model for FRP-confined concrete. Construct Build Mater. 2003;17(6–7):471–89.
40. Mandal S, Hoskin A, Fam A. Influence of concrete strength on confinement effectiveness of fiber-reinforced polymer circular jackets. ACI Struct J. 2005;102(3):383.
41. Cui C, Sheikh S. Experimental study of normal-and high-strength concrete confined with fiber-reinforced polymers. J Compos Construct. 2010;14(5):553–61.
42. Cui C, Sheikh S. Analytical model for circular normal- and high-strength concrete columns confined with FRP. J Compos Construct. 2010;14(5):562–72.
43. Li J, Wu C, Hao H. An experimental and numerical study of reinforced ultra-high performance concrete slabs under blast loads. Mater Des. 2015;82:64–76.
44. Thomas RJ, Sorensen AD. Review of strain rate effects for UHPC in tension. Construct Build Mater. 2017;153:846–56.
45. Zhu Y, Zhang Y, Hussein HH, Chen G. Flexural strengthening of reinforced concrete beams or slabs using ultra-high performance concrete (UHPC): a state of the art review. Eng Struct. 2020;205:110035.

46. Bajaber M, Hakeem I. UHPC evolution, development, and utilization in construction: a review. J Mater Res Technol. 2021; 10:1058–74.
47. Kadhim MM, Saleh AR, Cunningham LS, Semendary AA. Numerical investigation of non-shear-reinforced UHPC hybrid flat slabs subject to punching shear. Eng Struct. 2021; 241:112444.
48. Yoo D-Y, Banthia N. Mechanical properties of ultra-high-performance fiber-reinforced concrete: a review. Cem Concr Compos. 2016;73:267–80.
49. Abbas S, Soliman AM, Nehdi ML. Exploring mechanical and durability properties of ultra-high performance concrete incorporating various steel fiber lengths and dosages. Construct Build Mater. 2015;75:429–41.
50. Singh M, Sheikh AH, Mohamed Ali MS, Visintin P, Griffith MC. Experimental and numerical study of the flexural behaviour of ultra-high performance fibre reinforced concrete beams. Construct Build Mater. 2017;138:12–25.
51. Shafieifar M, Farzad M, Azizinamini A. Experimental and numerical study on mechanical properties of ultra high performance concrete (UHPC). Construct Build Mater. 2017;156:402–11.
52. Wu Z, Shi C, He W, Wang D. Uniaxial compression behavior of ultra-high performance concrete with hybrid steel fiber. J Mater Civil Eng. 2016;28(12):6016017.
53. Katlav M, Ergen F. Improved forecasting of the compressive strength of ultra-high-performance concrete (UHPC) via the CatBoost model optimized with different algorithms. Struct Concr. 2025;26(1):212–35.
54. Zheng H, Luo G, Yan K, Zhou D, Song C, Li Y. Mechanical performance of UHPC waffle plate under local loading: an experimental study. Struct Concr. 2025:1–13. https://doi.org/10.1002/suco.202400814
55. Wang Q, Liang XH, Liu X, Guo SP, Lu CL. Axial compressive performance of RC columns strengthened with prestressed CFRP fabric and UHPC jacket with spiral stirrups. Struct Concr. 2025;26(1):697–719.
56. Deng S, Huang Z, Yan B, Shen L, Huang Z, Wang Y. Experimental study and optimal design of UHPC T-shaped beam. Struct Concr. 2024;25(2):992–1005.
57. Al-Osta MA, Kharma KM, Ahmad S, Maslehuddin M, Al-Huri M, Khalid H. Strategies for strengthening of corroded reinforced concrete beams using CFRP laminates and UHPC jacketing. Struct Concr. 2023;24(1):1546–71.
58. Zhang X, Chen B, Zheng Z, Liu X, Chen Z, Cao J, et al. Strain distribution prediction in UHPC beams using deep learning model. Struct Concr. 2025;26(1):643–57.
59. Alsomiri M, Liu Z, Wang T, Meng J. Ductility-oriented design of UHPC T-beams: mechanical model and design recommendations. Struct Concr. 2025;26(1):425–48.
60. Tayeh B, Hadzima-Nyarko M, Riad MYR, Hafez RDA. Behavior of ultra-high-performance concrete with hybrid synthetic fiber waste exposed to elevated temperatures. Buildings. 2023; 13(1):129.
61. Haido JH, Abdul-Razzak AA, Al-Tayeb MM, Bakar BHA, Yousif ST, Tayeh BA. Dynamic response of reinforced concrete members incorporating steel fibers with different aspect ratios. Adv Concr Construct. 2021;11(2):89–98.
62. Tayeh BA, Aadi AS, Hilal N, Bakar BHA. Properties of ultra-high-performance fiber-reinforced concrete (UHPFRC)—a review paper. AIP Conference Proceedings. USA: AIP Publishing LLC; 2019.
63. Yu R, Spiesz P, Brouwers H. Mix design and properties assessment of ultra-high performance fibre reinforced concrete (UHPFRC). Cem Concr Res. 2014;56:29–39.
64. Yu R, Spiesz P, Brouwers H. Development of ultra-high performance fibre reinforced concrete (UHPFRC): towards an efficient utilization of binders and fibres. Construct Build Mater. 2015;79:273–82.
65. Wang D, Shi C, Wu Z, Xiao J, Huang Z, Fang Z. A review on ultra high performance concrete: part II. Hydration, microstructure and properties. Construct Build Mater. 2015;96:368–77.
66. Shi C, Wu Z, Xiao J, Wang D, Huang Z, Fang Z. A review on ultra high performance concrete: part I. Raw materials and mixture design. Construct Build Mater. 2015;101:741–51.
67. Wang C, Yang C, Liu F, Wan C, Pu X. Preparation of ultra-high performance concrete with common technology and materials. Cem Concr Compos. 2012;34(4):538–44.
68. Wille K, Naaman AE, Parra-Montesinos GJ. Ultra-high performance concrete with compressive strength exceeding 150 MPa (22 ksi): a simpler way. ACI Mater J. 2011;108(1):46.
69. Alkaysi M, el-Tawil S, Liu Z, Hansen W. Effects of silica powder and cement type on durability of ultra high performance concrete (UHPC). Cem Concr Compos. 2016;66:47–56.
70. Hajar Z. Design and construction of the world first ultra-high performance concrete road bridges. Proceedings of the Int. Symp. on UHPC, Kassel, Germany. 2004.
71. Gu C, Ye G, Sun W. Ultrahigh performance concrete-properties, applications and perspectives. Sci China Technol Sci. 2015;58:587–99.
72. Lopez JA, Serna P, Camacho E, Coll H, Navarro-Gregori J. First ultra-high-performance fibre-reinforced concrete footbridge in Spain: design and construction. Struct Eng Int. 2014; 24(1):101–4.
73. Shin H-O, Min K-H, Mitchell D. Confinement of ultra-high-performance fiber reinforced concrete columns. Compos Struct. 2017;176:124–42.
74. Yang X, Zohrevand P, Mirmiran A. Behavior of ultrahigh-performance concrete confined by steel. J Mater Civil Eng. 2016;28(10):4016113.
75. Benjamin AG. Characterization of the behavior of ultra-high performance concrete. Washington, DC: The University of Maryland; 2005. p. 300–70.
76. Pan B, Liu F, Zhuge Y, Zeng JJ, Liao JJ. ECCs/UHPFRCCs with and without FRP reinforcement for structural strengthening/repairing: a state-of-the-art review. Construct Build Mater. 2022;316:125824.
77. Cao S, Wu C, Wang W. Behavior of FRP confined UHPFRC-filled steel tube columns under axial compressive loading. J Build Eng. 2020;32:101511.
78. Eid R, Paultre P. Compressive behavior of FRP-confined reinforced concrete columns. Eng Struct. 2017;132:518–30.
79. Guo Y-C, Ye YY, Guan-Lin L, Lv JF, Bai YL, Zeng JJ. Effective usage of high strength steel tubes: axial compressive behavior of hybrid FRP-concrete-steel solid columns. Thin-Walled Struct. 2020;154:106796.
80. Lin G, Zeng JJ, Teng JG, Li LJ. Behavior of large-scale FRP-confined rectangular RC columns under eccentric compression. Eng Struct. 2020;216:110759.

81. De Luca A, Nardone F, Matta F, Nanni A, Lignola GP, Prota A. Structural evaluation of full-scale FRP-confined reinforced concrete columns. J Compos Construct. 2011;15(1):112–23.
82. Bisby L, Ranger M. Axial–flexural interaction in circular FRP-confined reinforced concrete columns. Construct Build Mater. 2010;24(9):1672–81.
83. Wang Z, Wang D, Smith ST, Lu D. Experimental testing and analytical modeling of CFRP-confined large circular RC columns subjected to cyclic axial compression. Eng Struct. 2012;40:64–74.
84. Mai AD, Sheikh MN, Hadi MN. Investigation on the behaviour of partial wrapping in comparison with full wrapping of square RC columns under different loading conditions. Construct Build Mater. 2018;168:153–68.
85. Isleem HF, Wang D, Wang Z. Modeling the axial compressive stress–strain behavior of CFRP-confined rectangular RC columns under monotonic and cyclic loading. Compos Struct. 2018;185:229–40.
86. Zohrevand P, Mirmiran A. Behavior of ultrahigh-performance concrete confined by fiber-reinforced polymers. J Mater Civil Eng. 2011;23(12):1727–34.
87. Guler S. Axial behavior of FRP-wrapped circular ultra-high performance concrete specimens. Struct Eng Mech. 2014;50(6):709–22.
88. Deng Z-c, Qu J-l. The experimental studies on behavior of ultrahigh-performance concrete confined by hybrid fiber-reinforced polymer tubes. Adv Mater Sci Eng. 2015;2015(1):201289.
89. Wang W, Wu C, Liu Z, Si H. Compressive behavior of ultra-high performance fiber-reinforced concrete (UHPFRC) confined with FRP. Compos Struct. 2018;204:419–37.
90. Tian H, Zhou Z, Wei Y, Wang Y, Lu J. Experimental investigation on axial compressive behavior of ultra-high performance concrete (UHPC) filled glass FRP tubes. Construct Build Mater. 2019;225:678–91.
91. de Oliveira DS, Raiz V, Carrazedo R. Experimental study on normal-strength, high-strength and ultrahigh-strength concrete confined by carbon and glass FRP laminates. J Compos Constr. 2019;23(1):4018072.
92. Liao J, Yang KY, Zeng JJ, Quach WM, Ye YY, Zhang L. Compressive behavior of FRP-confined ultra-high performance concrete (UHPC) in circular columns. Eng Struct. 2021;249:113246.
93. Ding Y, Zhou Z, Tian H, Peng Z. Compressive behavior of concrete-filled ultra-high performance concrete tube with FRP stirrups. Structure. 2022;46:611.
94. Huang L, Su L, Xie J, Lu Z, Li P, Hu R, et al. Dynamic splitting behaviour of ultra-high-performance concrete confined with carbon-fibre-reinforced polymer. Compos Struct. 2022;284:115155.
95. Tian H, Zhou Z, Li B, Jiang C. Effect of strain gradient on the stress–strain relationship of FRP-confined ultra-high performance concrete. Compos Struct. 2023;304:116371.
96. Wang J, Zhang SS, Nie XF, Yu T. Compressive behavior of FRP-confined ultra-high performance concrete (UHPC) and ultra-high performance fiber reinforced concrete (UHPFRC). Compos Struct. 2023;312:116879.
97. Li W, Li W, Lu Y, Hu B, Zhou Y, Wu H, et al. Axial compressive behavior and failure mechanism of CFRP partially confined ultra-high performance concrete (UHPC). Construct Build Mater. 2024;426:136104.
98. Wang J, Nie XF, Yang L, Li WG, Zhang SS. Compressive behavior of FRP-UHPC-steel double-skin tubular columns. Eng Struct. 2025;325:119451.
99. Su Y, Li J, Wu C, Wu P, Li ZX. Influences of nano-particles on dynamic strength of ultra-high performance concrete. Compos Part B Eng. 2016;91:595–609.
100. Gomez J, Shukla A, Sharma A. Static and dynamic behavior of concrete and granite in tension with damage. Theor Appl Fract Mech. 2001;36(1):37–49.
101. Liu P, Zhou X, Qian Q, Berto F, Zhou L. Dynamic splitting tensile properties of concrete and cement mortar. Fatigue Fract Eng Mater Struct. 2020;43(4):757–70.
102. Cadoni E, Forni D. Experimental analysis of the UHPFRCs behavior under tension at high stress rate. Eur Phys J Spec Top. 2016;225(2):253–64.
103. Su Y, Li J, Wu C, Wu P, Li ZX. Effects of steel fibres on dynamic strength of UHPC. Construct Build Mater. 2016;114:708–18.
104. Ozbakkaloglu T. Compressive behavior of concrete-filled FRP tube columns: assessment of critical column parameters. Eng Struct. 2013;51:188–99.
105. Ozbakkaloglu T. Behavior of square and rectangular ultra high-strength concrete-filled FRP tubes under axial compression. Compos Part B Eng. 2013;54:97–111.
106. Yoo D-Y, Banthia N, Kang ST, Yoon YS. Size effect in ultra-high-performance concrete beams. Eng Fract Mech. 2016;157:86–106.
107. Mirmiran A, Shahawy M, Beitleman T. Slenderness limit for hybrid FRP-concrete columns. J Compos Construct. 2001;5(1):26–34.
108. Huang L, Xie J, Li L, Xu B, Huang P, Lu Z. Compressive behaviour and modelling of CFRP-confined ultra-high performance concrete under cyclic loads. Construct Build Mater. 2021;310:124949.
109. Vincent T, Ozbakkaloglu T. Influence of fiber orientation and specimen end condition on axial compressive behavior of FRP-confined concrete. Construct Build Mater. 2013;47:814–26.
110. Sadeghian P, Rahai AR, Ehsani MR. Effect of fiber orientation on compressive behavior of CFRP-confined concrete columns. J Reinf Plast Compos. 2010;29(9):1335–46.
111. Zeng J-J, Feng P, Dai JG, Zhuge Y. Development and behavior of novel FRP-UHPC tubular members. Eng Struct. 2022;266:114540.
112. Liao J, Zeng JJ, Gong QM, Quach WM, Gao WY, Zhang L. Design-oriented stress–strain model for FRP-confined ultra-high performance concrete (UHPC). Construct Build Mater. 2022;318:126200.
113. Wang X, Wang R, Zhu Z, Wang K. Study on flexural capacity of UHPC-NC composite slab with reinforced truss in the Normal section. Buildings. 2024;14:3732. https://doi.org/10.3390/buildings14123732
114. Zeng J-J, Su TH, Chen JD, Hu X, Ng CT, Zheng Y, et al. Novel prefabricated FRP bar reinforced UHPC shells for column strengthening: development and axial compression tests. J Build Eng. 2024;94:109935.

AUTHOR BIOGRAPHIES

Rami J. A. Hamad, Associate Professor, Department of Facilities and Construction Project Management, International College of Engineering and Management affiliated with the University of Central Lancashire (UK), P.C. 111, Muscat, Oman. Email: rami@icem.edu.om

Mustafa Maher Al-Tayeb, Associate Professor, Department of Civil Engineering, Faculty of Engineering, Hasan Kalyoncu University, Şahinbey, Gaziantep, Turkey. Email: mustafa.altayeb@hku.edu.tr

Bassam A. Tayeh, Professor, Civil Engineering Department, Faculty of Engineering, Islamic University of Gaza, Palestine. Email: btayeh@iugaza.edu.ps

Majed A. A. Aldahdooh, Associate Professor, Department of Facilities and Construction Project Management, International College of Engineering and Management affiliated with the University of Central Lancashire (UK), P.C. 111, Muscat, Oman. Email: majidaldahdooh@icem.edu.om

Nurdeen M. Altwair, Professor, Civil Engineering Department, Faculty of Engineering, Elmergib University, Khoms, Libya. Email: nmaltwair@elmergib.edu.ly

Abdullah M. Zeyad, Civil Engineering, College of Engineering, Jazan University, 45142 Jazan, Saudi Arabia. Email: azmohsen@jazanu.edu.sa

How to cite this article: Hamad RJA, Al-Tayeb MM, Tayeh BA, Aldahdooh MAA, Altwair NM, Zeyad AM. A review on the behavior of FRP-reinforced ultra-high-performance concrete tubes. Structural Concrete. 2025. https://doi.org/10.1002/suco.70330